Research Article

Efficiency of dynamic relaxation methods in form-finding of tensile membrane structures

Mohsen Khatibinia[1] · Saeed Hosseinaei[1] · Seyyed Reza Sarafrazi[1]

Abstract

The main idea of this study is to investigate and compare the efficiency of the dynamic relaxation methods (DRMs) in the form-finding of tensile membrane structures (TMSs). The form-finding process as a main stage in the design and construction of TMSs has been considered for finding an equilibrium configuration subjected to a specific prestress distribution. DRMs as a pseudo-dynamic analysis are an explicit iterative technique for the nonlinear analysis of structures. In the techniques, the static equilibrium of structures is solved by integrating the pseudo-dynamic equations in order to obtain the steady state of the pseudo-dynamic problem. In this study, the efficiency and generality performance of DRMs are compared through solving three selected TMSs. In order to achieve this purpose, seven schemes of the DR approach are selected based on combining the fictitious parameters including the time step, diagonal mass, and damping matrices which were proposed in the previous studies. Furthermore, a reference index is proposed by combining the total number of iterations and the overall duration of analysis in order to appropriately compare the schemes of the DR approach in the form-finding of TMSs.

Keywords Tensile membrane structures · Dynamic relaxation method · Form-finding · Nonlinear analysis · Reference index

1 Introduction

Tensile membrane structures (TMSs) are well known as lightweight and cost-effective structures that are used for long span roofing components, such as buildings, stadiums, and exhibition halls. Along with structural stability, TMS(s) attain an aesthetic architectural form [1, 2]. The coated fabrics utilized in the construction of a TMS are unable to resist flexure and shear forces. However, these materials can reduce not only temperature but also the costs of maintenance due to their self-cleaning properties. Such structures are able to tolerate external events through their membrane prestress in plane and anticlastic surface curvature. TMSs in comparison with traditional roofing materials also bear a lower structural load and more earthquake resistance produce due to the membrane's elasticity.

The stages of form-finding, static analysis, and patterning are considered as the preliminary design procedure of a TMS [3]. Furthermore, the initial design of a TMS includes of two primary steps: (1) determining an equilibrium form of a TMS and (2) implementing analysis of the form subjected to its service condition loads [4].

The surface geometry (i.e., form) of a TMS is not known a priori and so poses a challenge for designers. Hence, the form-finding process can determine the optimal form of structures which then satisfies the constraints of both architectural and mechanical requirements. To find the optimal form of a TMS with given boundary conditions, an initial prestress load is applied in both directions including the warp and fill yarns in the fabric. A unique shape, an equilibrium stress state subjected to the prestress load and defined boundary conditions are adopted for the flexible

---
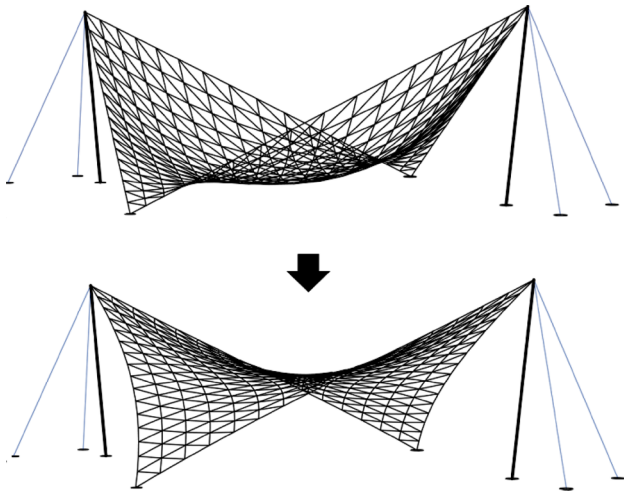
Fig. 1 Form-finding of a TMS. Starting with the geometry at the top and ending up with the form-found hypar, at the bottom, where all nodes are in equilibrium

surface. Figure 1 provides an example of the form-finding process.

In order to implement the form-finding process, several numerical methods have been proposed, such as the force density (FD) method [5], dynamic relaxation method (DRM) [6, 7], updated reference strategy [8] and particle spring systems [9]. At first, these methods were adopted and developed for implementing the form-finding of pre-stressed membrane structures. In recent years, significant methods have been developed and several improvements have been proposed. To find the equilibrium form of membrane structures, Sheck [10] introduced a simple linear method based on force densities. In this method, it was assumed that a structure can be modeled and considered by cable networks. Employing the surface stress density method as an iterative procedure, Maurin and Motro [11] proposed a new form-finding method for TMSs. In the surface stress density method, an isotropic stress tensor and an iterative procedure were considered for triangular elements. By achieving the convergence of the procedure, configurations were concluded that satisfy the conditions of the static equilibrium laws. Sanchez et al. [12] presented a novel approach for the conceptual design of fabric tensile structures. In order to obtain preliminary shapes of tensile structures, the proposed approach combined a form-finding method with a surface fitting approach. With the FD method, the value of force density often depends on the researcher's experience and can only be determined after several trial calculations. Hence, Ye et al. [13] introduced a modified FD approach for the form-finding of membrane structures. According to their method, membrane stress and cable tension were utilized as initial conditions instead of as the assumed value of FD approach (i.e., the

quantitative relationships between membrane stress, cable tension, and force density were established), and the unbalanced force of each node was employed to control the error. Barnes [14] described a DRM-based numerical procedure with kinetic damping (called the kinetic DRM) for the form-finding, analysis, and fabrication patterning of TMDs. In the kinetic DRM, damping factor is equal to zero. Passing from a peak point of the kinetic energy diagram indicates that the kinetic energy has a reducing trend. Using the result of this time leads to divergence process. From the viewpoint of a practicing membrane engineer, Wakefield [7] reviewed the selection and application of appropriate analysis techniques and demonstrated that DRM may be considered as the preferred form-finding method. Lewis [15] discussed the advantages and limitations of three approaches, namely transient stiffness, FD, and DRM. In addition, the study provided insight into their applicability as the numerical tools of design in fabric structures. Recently, Alic and Persson [16] introduced a form-finding method established by a hybrid of DRM and isogeometric membrane elements. The elements were developed based on non-uniform rational B-splines (NURBS). The results of this study revealed that the discretization and shape of elements effectively impressed on the form-finding. This procedure can be used to quickly find form-finding since, in NURBS' description of the curved geometry well, form-finding may be performed with a coarse mesh. Other engineering problems have also demonstrated the successful application of isogeometric analysis [17, 18].

The main contribution of the present study is to investigate the effectiveness of different DRM-based strategies in the form-finding of TMSs. In the DRM techniques, the fictitious mass, damping, and time step factors impress on their stability and speed of convergence. Hence, the efficiency and generality performance of DRMs based on combining the proposed fictitious parameters including the time step, diagonal mass, and damping matrices are compared through solving three selected TMSs. Furthermore, a reference index as an efficient criterion is proposed by the combination of the total number of iterations and overall analysis duration. The results show that the reference index can be adopted for comparing the generality performance of DRMs. In addition, the DR approaches can be efficiently used as a suitable tool in the form-finding of TMSs.

2 Standard dynamic relaxation approach

Day [19] first introduced the dynamic relaxation (DR) approach whose theory was developed and details presented in the studies by Barnes [6], Lewis [1], and Topping and Ivanyi [20]. In the finite element method, the vector of

displacements **X** can be obtained through the vector of nodal loads **P** and structural stiffness matrix **S**, as follows:

$$\mathbf{SX} = \mathbf{P} \tag{1}$$

In the nonlinear analysis of structures, the stiffness matrix **S(X)** is expressed as a function of displacements. The nonlinear system of structures can be solved by an iterative procedure. Hence, DRM was introduced as an explicit iterative technique for this purpose. In the DR technique, the static state of Eq. (1) is converted into the artificial dynamic state by adding artificial fictitious inertial and damping forces, as follows:

$$\mathbf{M}^n\ddot{\mathbf{X}}^n + \mathbf{C}^n\dot{\mathbf{X}}^n + \mathbf{S}^n\mathbf{X}^n = \mathbf{P}^n \tag{2}$$

where $\mathbf{M}^n$ and $\mathbf{C}^n$ are the fictitious mass and damping matrices in the nth iteration of DRM, respectively. $\ddot{\mathbf{X}}^n$ and $\dot{\mathbf{X}}^n$ are the acceleration and velocity vectors in the nth iteration of DRM, respectively. For the simplicity of this method, the matrices are always assumed as a diagonal matrix.

The DR technique was formulated based on the second-order Richardson method and was considered as the response of the steady state in an artificially dynamic system [21]. The fundamental relationships of the explicit DRM are obtained by the central finite difference technique as follows [22]:

$$\dot{x}_i^{n+\frac{1}{2}} = \frac{2m_{ii}^n - t^n c_{ii}^n}{2m_{ii}^n + t^n c_{ii}^n}\dot{x}_i^{n-\frac{1}{2}} + \frac{2t^n}{2m_{ii}^n + t^n c_{ii}^n}r_i^n; \quad i = 1, 2, \ldots, q \tag{3}$$

$$x_i^{n+1} = x_i^n + t^{n+1}\dot{x}_i^{n+\frac{1}{2}}; \quad i = 1, 2, \ldots, q \tag{4}$$

where t^n, m_{ii}^n and c_{ii}^n are considered as the fictitious time step, ith diagonal element of fictitious mass, and damping matrices in the nth iteration of DRM, respectively. Also, q is the number of degrees of freedom and r_i^n is the residual force of the ith degree of freedom. The vector of the residual force $\mathbf{R}^n$ is defined in the nth iteration as:

$$\mathbf{R}^n = \mathbf{M}^n\ddot{\mathbf{X}}^n + \mathbf{C}^n\dot{\mathbf{X}}^n = \mathbf{P}^n - \mathbf{f}^n \tag{5}$$

In order to achieve the numerical stability of the DR approach, the fictitious matrix **M** is calculated based on the Gershgorin theorem as follows [22]:

$$m_{ii}^n > \frac{(t^n)^2}{4}\sum_{j=1}^{q}\left|s_{ij}^n\right|; \quad i = 1, 2, \ldots, q \tag{6}$$

Furthermore, the critical damping is obtained for fictitious damping as follows:

$$c_{ii}^n = 2\omega_{\min}m_{ii}^n; \quad i = 1, 2, \ldots, q \tag{7}$$

where $\omega_{\min}$ is the lowest frequency of structure, which is calculated based on the Rayleigh principle:

$$\omega_{\min}^2 = \frac{(\mathbf{X}^n)^{\mathrm{T}}\mathbf{f}^n}{(\mathbf{X}^n)^{\mathrm{T}}\mathbf{M}^n\mathbf{X}^n} \tag{8}$$

By assigning an acceptable residual error, ε, the DRM can be converged to the solution of Eq. (1). Therefore, the algorithm of the DRM can be expressed as:

(1) Defining $\varepsilon, \mathbf{X}^0, \dot{\mathbf{X}}^{-1/2} = \mathbf{0}$ and t^0.
(2) $n = 0$.
(3) Calculating the internal force vector and applying boundary conditions.
(4) Determining the residual forces, artificial mass and damping matrices.
(5) Updating the time step t.
(6) Calculating $\dot{\mathbf{X}}^{n+1/2}$ and $\mathbf{X}^{n+1}$.
(7) If $\left\|\mathbf{R}^{n+1}\right\| \le \varepsilon$, stop the DR algorithm.
(8) $n = n + 1$.
(9) If $n \le n_{\max}$, continue the iteration of the DRM from the step (3).

3 Modifications of the standard DRM

The iterations are inherently unstable in the standard DRM because the numerical time integration is utilized for solving the differential equations of motion [23–26]. Hence, the stability of DRM depends on fictitious parameters including the time step, diagonal mass, and damping matrices. Therefore, new techniques have been proposed for calculating these fictitious parameters. In the following section, some of the selected techniques are expressed.

3.1 Optimal time step

Kadkhodayan et al. [27] proposed an optimal time step based on minimizing residual forces. In this study, the following relation was introduced for the rate reduction in the nodal residual forces' sum of squares, Z_R:

$$\sum_{i=1}^{q}\left(p_i^{n+1} - f_i^{n+1}\right)^2 \le Z_R\sum_{i=1}^{q}\left(r_i^n\right)^2 \tag{9}$$

The following internal forces at time $t_n + \Delta t$ are also obtained using the finite difference technique:

$$f_i^{n+1} = f_i^n + t^{n+1}\dot{f}_i^{n+1/2} \tag{10}$$

In Eq. (10), the rate of changes in the internal forces (i.e., $\dot{f}^{n+1/2}$) is approximately assumed to be $\sum_{j=1}^{q}s_{ij}\dot{x}_j^{n+1/2}$. By

the minimization of parameter Z_R, the optimum time step is obtained as:

$$t^{n+1} = \frac{\sum_{i=1}^{q} r_i^n \dot{f}_i^{n+\frac{1}{2}}}{\sum_{i=1}^{q} \left(\dot{f}_i^{n+\frac{1}{2}} \right)^2} \tag{11}$$

It should be noted that the second-order derivative of Z_R with respect to t^{n+1} is always positive so that Eq. (11) produces the highest convergence rate. Sometimes, an extremely small or a very large value is obtained for the time step, which may cause numerical instability [25].

3.2 The modified DRM

Rezaiee-Pajand and Alamatian [23] proposed a modified DRM, called mdDR, based on minimizing the error of displacement between two iterations in which DRM obtains the convergence. In the mdDR technique, the new formulas were proposed for the fictitious mass and damping. In the nth iteration of the DR technique, the displacement error can be defined as follows:

$$\mathbf{e}^n = \mathbf{X}^n - \mathbf{X}^* \tag{12}$$

where X^* is the answer of Eq. (1).

By minimizing the displacement error and assuming the constant value for the fictitious time step, the fictitious mass is defined as follows:

$$m_{ii}^n = \max \left\{ \frac{(t^n)^2}{2} s_{ii}^n, \frac{(t^n)^2}{4} \sum_{j=1}^{q} \left| s_{ij}^n \right| \right\}; \quad i = 1, 2, \ldots, q \tag{13}$$

For each of freedom degrees, the diagonal elements of the fictitious damping matrix are also determined as [21]:

$$c_{ii}^n = m_{ii}^n \sqrt{\omega_{\min}^2 \left[4 - (t^n)^2 \omega_{\min}^2 \right]}; \quad i = 1, 2, \ldots, q \tag{14}$$

In fact, the mdDR technique can enhance the convergence rate of DRM and can reduce its computational cost [23].

3.3 Fictitious damping factor technique

The artificial damping factor is presented as the lowest eigenvalue (or minimum frequency) of the artificial dynamic system. Furthermore, many researches have employed the Rayleigh principle for obtaining the upper bound of the lowest eigenvalue, $\lambda_{\min}$. Thus, the quick convergence of the DR technique can be obtained by exploiting a better evaluation of $\lambda_{\min}$ [24]. Based on this concept, Rezaiee-Pajand and Sarafrazi [21] and Sarafrazi [28] proposed a new scheme for finding $\lambda_{\min}$, which used a combined step from the power

iterative scheme. In fact, the power iterative process can converge on the highest eigenvalue. Assuming a as the upper bound of the highest eigenvalue, the lowest eigenvalue of $\mathbf{M}^{-1}\mathbf{S}$ can be obtained by applying the power iterative method on the matrix $[\mathbf{M}^{-1}\mathbf{S} - a\mathbf{I}]$. The works by Rezaiee-Pajand and Sarafrazi [21] and Sarafrazi [27] demonstrated that this approach is superior than the modified DRM for selection of the fictitious mass, i.e., Equation (13). Therefore, Rezaiee-Pajand and Sarafrazi [21] introduced this strategy for updating the damping factor as:

$$\mathbf{v}^n = \mathbf{M}^{-1}\mathbf{S}\mathbf{u}^n - a\mathbf{I}\mathbf{u}^n; \quad \lambda^n = \max(\mathbf{v}^n); \quad \mathbf{u}^{n+1} = \mathbf{v}^n / \lambda^n \tag{15}$$

$$\lambda_1^n = \lambda^n + a; \quad c^n = \sqrt{\lambda_1^n (4 - \lambda_1^n)} \tag{16}$$

where $\mathbf{u}$ is the eigenvector of $\mathbf{M}^{-1}\mathbf{S}$. This proposed scheme is started from $\mathbf{u}^0 = \mathbf{I}$ and $\lambda^0 = 1$.

It should be noted that the lowest eigenvalue is first obtained from Eq. (16) and is compared with that of Rayleigh concept. Finally, the minimum value is utilized for updating the artificial damping factor.

3.4 Residual energy minimizer time step

By minimizing the unbalanced energy function in each iteration, Rezaiee-Pajand et al. [25] introduced a new fictitious time step. Based on their study, the residual energy of a structural system can be expressed as a function from the residual force and displacement vectors. Thus, in the $n+1$th iteration of the DR technique, this function (i.e., UBE) is obtained from the following formula:

$$\text{UBE} = \sum_{i=1}^{q} \left(\delta \mathbf{X}_i^{n+1} r_i^{n+1} \right)^2 \tag{17}$$

By replacing out-of-balance force from Eq. (5), the function UBE can be expressed as:

$$\text{UBE} = (t^{n+1})^2 \sum_{i=1}^{q} \left[\dot{x}_i^{n+1} (r_i^n - t^{n+1} \dot{f}_i^{n+1}) \right]^2 \tag{18}$$

Therefore, the unbalanced energy function defined in Eq. (18) is minimized respect to the time step and the following two values are concluded as:

$$t^{n+1} = \frac{-A_2^{n+1} \pm \sqrt{(A_2^{n+1})^2 - 4A_1^{n+1} A_3^{n+1}}}{2A_1^{n+1}} \tag{19}$$

where A_1^{n+1}, A_2^{n+1} and A_3^{n+1} are constant factors and can be obtained as:

$$A_1^{n+1} = 2 \sum_{i=1}^{q} \left(\dot{x}_i^{n+\frac{1}{2}} \dot{f}_i^{n+\frac{1}{2}} \right)^2 \tag{20}$$

$$A_2^{n+1} = -3 \sum_{i=1}^{q} \left(\dot{x}_i^{n+\frac{1}{2}} \right)^2 r_i^n \dot{f}_i^{n+\frac{1}{2}} \tag{21}$$

$$A_3^{n+1} = \sum_{i=1}^{q} \left(\dot{x}_i^{n+\frac{1}{2}} r_i^n \right)^2 \tag{22}$$

For minimizing the UBE function, the second-order derivative of UBE respect to the fictitious time step is greater than zero:

$$\frac{\partial^2 \text{UBE}}{\partial (t^{n+1})^2} > 0 \Rightarrow 2A_1^{n+1} t^{n+1} + A_2^{n+1} > 0 \tag{23}$$

Thus, one of two values of Eq. (19) is selected based on the satisfaction of the condition which is introduced in Eq. (23).

4 Finite element method for the nonlinear analysis of TMS

This section presents the finite element method for the nonlinear analysis of TMSs. For this purpose, the plane-stress triangular element is employed for describing three-dimensional membranes. Furthermore, the approach for obtaining the geometric stiffness matrix of membrane structures is presented.

4.1 The plane-stress triangular element

In this section, the stiffness matrix and force vector of the plane-stress triangular element (Fig. 2) are presented
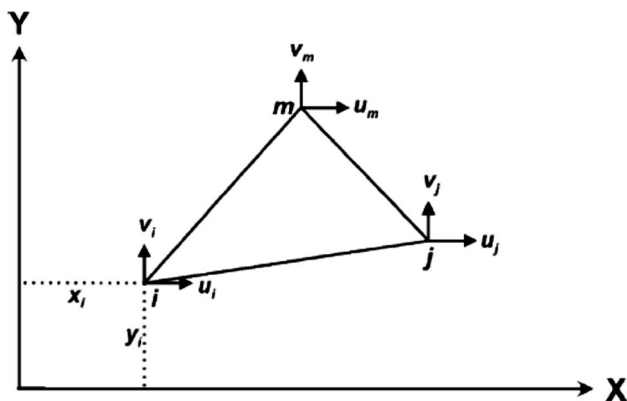

Fig. 2 Plane-stress triangular element

in the global 2-D coordinate system [29]. In this study, a local coordinate system is first assumed for each element in the 3-D membrane structures. It should be noted that this approach shall be referred to as the local coordinate system of the element.

As seen from Fig. 2, the displacement vector of the element nodes is expressed as:

$$\mathbf{a}^e = \left\{ u_i \ v_i \ u_j \ v_j \ u_m \ v_m \right\} \tag{24}$$

For the plane-stress case, a linearly elastic stiffness matrix as a constant matrix is obtained, which is a 6×6 two-dimensional stiffness matrix as [29]:

$$\mathbf{K}_{E,2D}^e = \begin{bmatrix} (\mathbf{K}_E^e)_{ii} & (\mathbf{K}_E^e)_{ij} & (\mathbf{K}_E^e)_{im} \\ (\mathbf{K}_E^e)_{ji} & (\mathbf{K}_E^e)_{jj} & (\mathbf{K}_E^e)_{jm} \\ (\mathbf{K}_E^e)_{mi} & (\mathbf{K}_E^e)_{mj} & (\mathbf{K}_E^e)_{mm} \end{bmatrix} \tag{25}$$

with

$$\begin{aligned} (\mathbf{K}_E^e)_{rs} = \ & \frac{h}{4A} \cdot \frac{E}{1-v^2} \\ & \times \begin{bmatrix} b_r b_s + \frac{1-v}{2} c_r c_s & v b_r b_s + \frac{1-v}{2} c_r b_s \\ v b_r b_s + \frac{1-v}{2} b_r c_s & c_r c_s + \frac{1-v}{2} b_r b_s \end{bmatrix}; \quad r,s = i,j,m \end{aligned} \tag{26}$$

where h and A are the thickness and area of the element, respectively. E and v are Young's modulus and Poisson's ratio of material. Also, the parameters of b and c are expressed as:

$$\begin{aligned} b_i &= y_j - y_m; & c_i &= x_m - x_j \\ b_j &= y_m - y_i; & c_j &= x_i - x_m \\ b_m &= y_i - y_j; & c_m &= x_j - x_i \end{aligned} \tag{27}$$

The nodal force vector for each element in the local coordinate system is also defined as:

$$\mathbf{F}^e = \frac{h}{2} \begin{Bmatrix} b_i \sigma_x + c_i \tau_{xy} \\ c_i \sigma_y + b_i \tau_{xy} \\ \vdots \\ b_j \sigma_x + c_j \tau_{xy} \\ c_j \sigma_y + b_j \tau_{xy} \\ \vdots \\ b_m \sigma_x + c_m \tau_{xy} \\ c_m \sigma_x + b_m \tau_{xy} \end{Bmatrix} = \frac{h}{2} \begin{Bmatrix} (\mathbf{F}_i)_x \\ (\mathbf{F}_i)_y \\ \vdots \\ (\mathbf{F}_j)_x \\ (\mathbf{F}_j)_y \\ \vdots \\ (\mathbf{F}_m)_x \\ (\mathbf{F}_m)_y \end{Bmatrix} \tag{28}$$

where σ_x, σ_y and τ_{xy} are the stresses of plane elasticity.

4.2 The geometric stiffness matrix of plane-stress triangular element

For each triangular element, a geometric stiffness matrix is defined based on the gradient of the nodal force vector $\mathbf{F}^e$ (Eq. 28) as [30]:

$$\mathbf{K}_{G,2D}^e = \begin{bmatrix} \mathbf{0} & \mathbf{A} & -\mathbf{A} \\ -\mathbf{A} & \mathbf{0} & \mathbf{A} \\ \mathbf{A} & -\mathbf{A} & \mathbf{0} \end{bmatrix} \qquad (29)$$

where

$$\mathbf{A} = \frac{h}{2} \begin{bmatrix} -\tau_{xy} & \sigma_x \\ -\sigma_y & \tau_{xy} \end{bmatrix} \qquad (30)$$

In fact, the explicit elastic and geometric stiffness matrices are provided by using Eqs. (25) and (30) for plane elasticity problems. In the next stage, three-dimensional rotational effects of each element should be considered. This issue is expressed in the following section presents.

4.3 Geometric stiffness matrix in 3-D space

The tangential stiffness matrix of a TMS includes of three components in the three-dimensional space. The elastic stiffness matrix is adopted as the first component and is obtained in the 2-D plane-stress stiffness based on Eq. (25). For this purpose, columns and rows of zeroes are added the stiffness matrix in the appropriate location. In fact, the columns and rows are assumed for the local z-coordinate. Based on the in-plane geometric stiffness matrix, the second component is obtained from the plane-stress stiffness matrix defined in Eq. (29). The out-of-plane geometric stiffness matrix is assumed as the third component and is expressed as the geometric effect. This component is

determined based on the approach introduced by Spillers et al. [30]. For describing the geometric effect, small rigid rotations are assumed and the change in the nodal force vector of element is computed in this approach. Hence, the geometric effect is constructed by using the relationship from rigid body mechanics [30]. According to the relationship, a small rigid body rotation shown by the vector $\boldsymbol{\omega}$ is first assumed, and then the change of vector $\mathbf{F}$ can be presented as:

$$d\mathbf{F} = \boldsymbol{\omega} \times \mathbf{F} = -\mathbf{F} \times \boldsymbol{\omega} \qquad (31)$$

Based on this approach, the out-of-plane stiffness matrix, K_G^e, to the geometric stiffness matrix in the local coordinate system (Fig. 3) is defined as follows:

$$\mathbf{K}_G^e = \frac{h}{2} \begin{bmatrix} (\mathbf{K}_G^e)_{ii} & (\mathbf{K}_G^e)_{ij} & (\mathbf{K}_G^e)_{im} \\ (\mathbf{K}_G^e)_{ji} & (\mathbf{K}_G^e)_{jj} & (\mathbf{K}_G^e)_{jm} \\ (\mathbf{K}_G^e)_{mi} & (\mathbf{K}_G^e)_{mj} & (\mathbf{K}_G^e)_{mm} \end{bmatrix} \qquad (32)$$
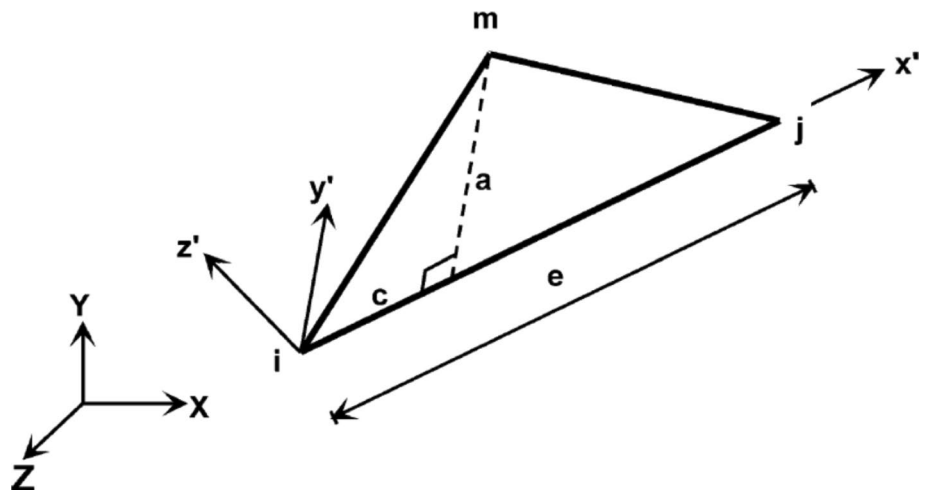
where

$$(\mathbf{K}_G^e)_{ri} = \begin{bmatrix} 0 & 0 & 0 \\ 0 & 0 & 0 \\ 0 & 0 & \alpha_r \end{bmatrix}; \quad (\mathbf{K}_G^e)_{rj} = \begin{bmatrix} 0 & 0 & 0 \\ 0 & 0 & 0 \\ 0 & 0 & \beta_r \end{bmatrix}; \quad (\mathbf{K}_G^e)_{rm} = \begin{bmatrix} 0 & 0 & 0 \\ 0 & 0 & 0 \\ 0 & 0 & \lambda_r \end{bmatrix} \qquad (33)$$

$$\alpha_r = -\frac{e-c}{ae}(\mathbf{F}_r)_{y'} - \frac{1}{e}(\mathbf{F}_r)_{x'}; \quad r = i,j,m \qquad (34)$$

$$\beta_r = -\frac{c}{ae}(\mathbf{F}_r)_{y'} - \frac{1}{e}(\mathbf{F}_r)_{x'}; \quad r = i,j,m \qquad (35)$$

$$\lambda_r = \frac{1}{a}(\mathbf{F}_r)_{y'}; \quad r = i,j,m \qquad (36)$$

Fig. 3 Triangular finite element in its local coordinate system [30]

Table 1 Schemes of the DR technique

Scheme	Fictitious parameters		
	Mass	Damping	Time
DRM 1	Equation (6)	Equation (7)	$t^k = 1$
DRM 2	Equation (6)	Equation (7)	Equation (11)
DRM 3	Equation (6)	Equation (7)	Equation (19)
DRM 4	Equation (13)	Equation (16)	$t^k = 1$
DRM 5	Equation (13)	Equation (7)	$t^k = 1$
DRM 6	Equation (13)	Equation (14)	$t^k = 1$
DRM 7	Equation (13)	Equation (16)	Equation (19)

The more detail of this approach can be found in Spillers et al. [30].

5 Form-finding procedure of TMS

In this study, the form-finding procedure of TMSs is presented using the DR approaches with the finite element theory mentioned above. For achieving this purpose, seven schemes of the DR approach are selected and their efficiency is compared in terms of the total number of iterations and the overall duration of analysis. In the schemes, the combination of DRM modifications are considered based on the combination of the fictitious time, mass, and damping which are presented in Sect. 3. The schemes are given in Table 1.

It is noted that the fourth and seventh schemes are proposed in this study. To compare the performance and efficiency of the schemes, the criteria proposed by Rezaiee-Pajand et al. [24] are used. The efficiency degree for the number of iterations, E_I^i, and the one related to the analysis duration, E_T^i, as the criteria are calculated as follows:

$$E_I^i = 100 \times \left(\frac{I_{max}^i - I^i}{I_{max}^i - I_{min}^i} \right) \tag{37}$$

$$E_T^i = 100 \times \left(\frac{T_{max}^i - T^i}{T_{max}^i - T_{min}^i} \right) \tag{38}$$

where I^i and T^i are the total number of iterations and the overall duration of analysis for $i$the DR scheme, respectively. According to the criteria, zero value represents the scheme with the highest number of iterations (or the analysis duration is high). In other words, the grade 100 represents the DR technique with the lowest number of iteration and time [24].

In this study, a reference index (RI) is introduced by combining the criteria presented based Eqs. (37) and (38) in

order to obtain an overall comparison. The RI parameter is obtained by calculating the average of the criteria as:

$$RI = \frac{E_I^i + E_T^i}{2} \tag{39}$$

In fact, the criterion can be efficiently used as an appropriate and convenient criterion instead of two criteria. A higher value of the RI parameter represents the scheme with the highest performance.

6 Illustrative examples

The schemes of DRM shown in Table 1 were applied to three different examples. All DR schemes were programmed in FORTRAN and calculations were carried out on the computer with processor AMDE-450 1.65 GHz, 4 GB RAM. The acceptable residual error (i.e. ε) was same for all solutions and was assumed to be equal to 10^{-4}. In all examples, the structure was discretized using triangular elements, and the surface topology was defined by a trial shape which is used in the first step of the form-finding analysis .

6.1 Spherical cap

The spherical cap shown in Fig. 4 was considered as the first example. A Young's modulus of 10,000 ksi and a Poisson's ratio of 0.3 are assumed for the structure. The spherical cap has a radius of 4.76 in, a central angle of 10.9 degrees and a thickness of 0.01,576 in. The initial prestress
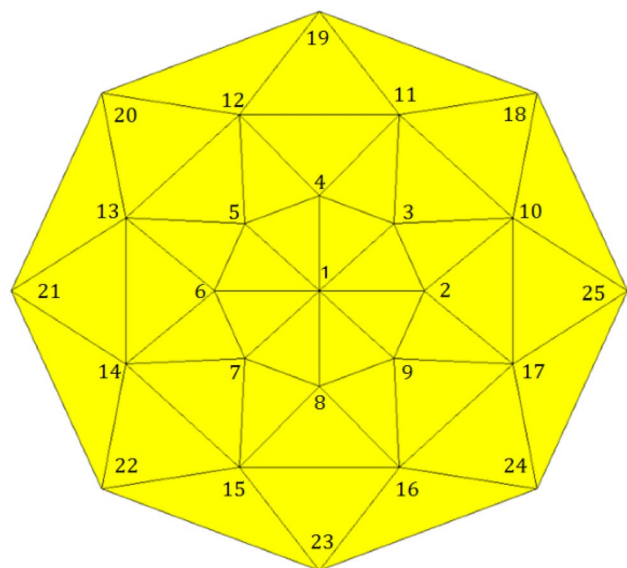

Fig. 4 Spherical cap

**Table 2** Comparing the results of the DR schemes for the loading condition Case 1

Scheme	Number of iterations in each loading step loading				I^i	E_I^i	$T^i(s)$	E_T^i	RI
	1	2	3	4					
DRM 1	63	57	55	54	229	0	1.41	22.97	11.48
DRM 2	33	27	28	31	119	100	1.04	72.97	86.48
DRM 3	31	33	31	36	131	89.09	0.84	100	94.55
DRM 4	38	35	36	38	147	74.54	1.26	43.24	58.89
DRM 5	60	55	53	52	220	8.18	1.58	0	4.09
DRM 6	54	50	48	47	199	27.27	0.92	89.18	58.22
DRM 7	30	36	42	39	147	74.54	0.84	100	87.27

Table 3 Comparing the results of the DR schemes for the loading condition Case 2

Scheme	Number of iterations in each loading step loading				I^i	E_I^i	$T^i(s)$	E_T^i	RI
	1	2	3	4					
DRM 1	41	39	39	41	160	6.25	1.04	38.63	22.44
DRM 2	37	39	38	38	152	56.25	1.05	36.36	46.310
DRM 3	39	38	40	41	158	18.75	1.21	0	9.38
DRM 4	41	38	41	41	161	0	0.96	56.81	28.41
DRM 5	36	35	36	40	145	100	0.87	77.27	88.63
DRM 6	37	38	38	38	151	62.50	0.77	100	81.25
DRM 7	38	36	38	38	150	68.75	1.00	47.72	58.23

values in the warp and fill directions is assumed equal to 2500 ksi. The form-finding of the structure is investigated subjected to two loading conditions: Case (1) 10 kip forces acting at nodes 1, 11, 12, 13, 14, 15, 16, and 17 along the negative Z-direction; and Case (2) 10 kip forces acting at nodes 1 to 17 along the negative Z-direction. The border nodes are fixed.

Tables 2 and 3 provide the results of the form-finding procedure for the two loading cases. The RI parameter is able to compare the DR schemes. As shown in Table 2, schemes 2, 3, 7 are the best techniques for solving the Case 1 loading condition. However, based on Table 3, for the Case 2 loading condition, it is obvious that schemes 5 and 6 are able to solve the form-finding of the structure.
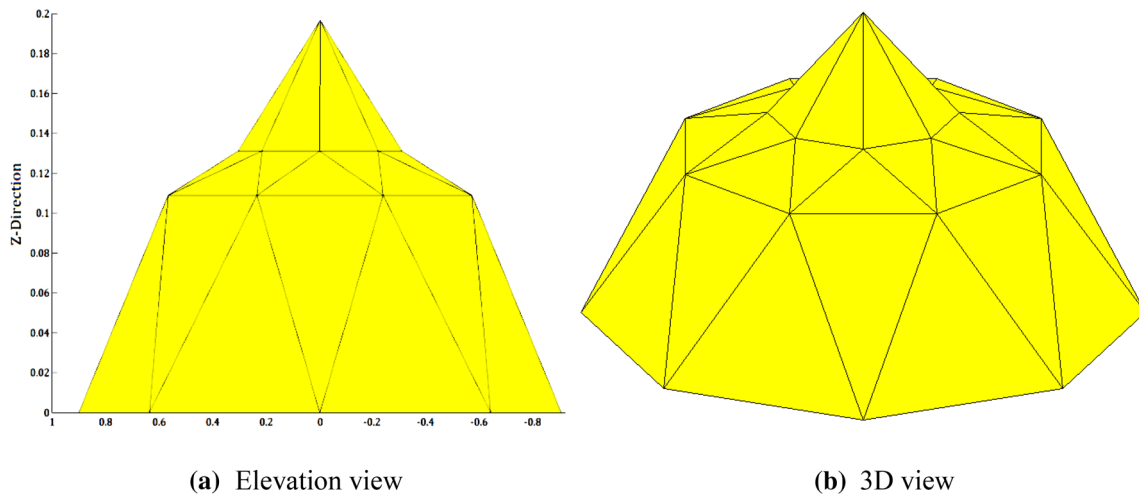
(a) Elevation view   **(b)** 3D view

Fig. 5 Form-finding model of the spherical cap subjected to the loading condition Case 1

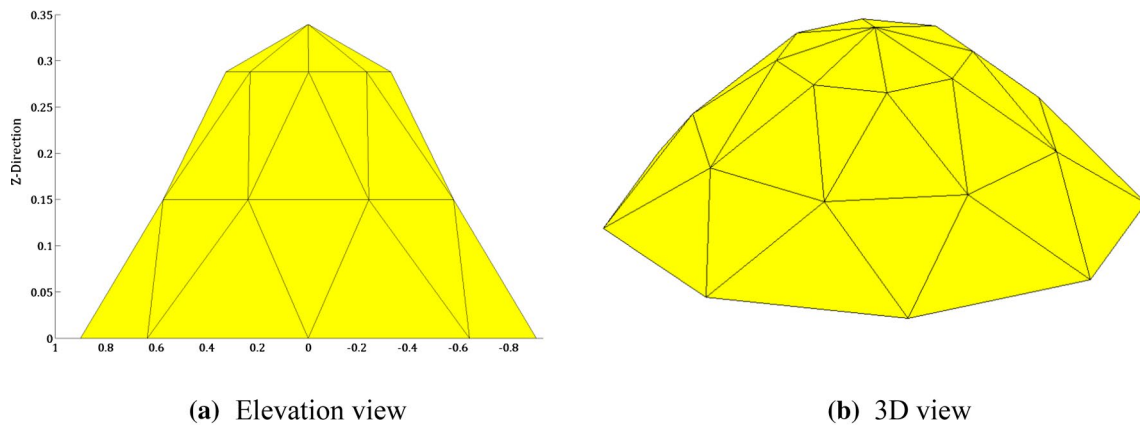**(a)** Elevation view   **(b)** 3D view

Fig. 6 Form-finding model of the spherical cap subjected to the loading condition Case 2
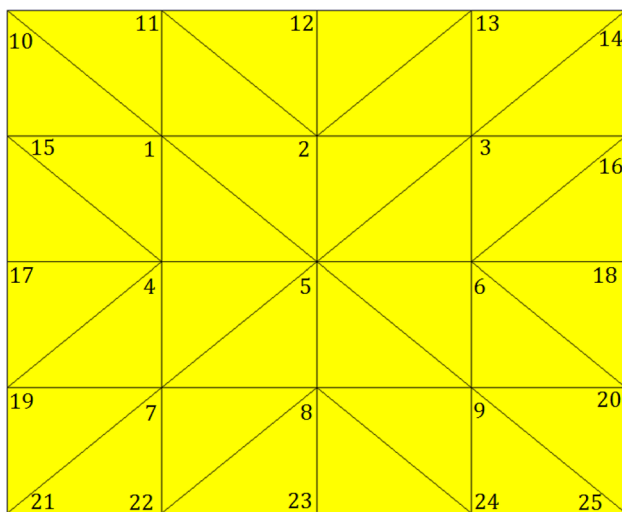

Fig. 7 Flat stretched membrane

For the membrane structure subjected to two loading conditions, the models of the form-finding obtained based on all DR schemes are same. The models are shown in Figs. 5 and 6.

6.2 A fat stretched membrane

The second test case is the flat stretched membrane shown in Fig. 7. The Young's modulus of material is 30,000 ksi and the Poisson's ratio is 0.3 for the flat stretched membrane. The thickness of this structure is set equal to 0.004167 in. The initial pre-stress values in the warp and fill directions is considered as 80 ksi. In this example, the form-finding procedure of the structure is subjected to two loading conditions: Case (1) 100 kip forces acting at nodes 1–9 along the negative Z-direction; and Case (2) 10 kip forces acting at nodes 2, 4, 5, 6 and 8 along the negative Z-direction. The border nodes as nodal supports are fixed.

For the two loading cases, Tables 4 and 5 compare the results of the DR schemes in the form-finding procedure. Tables 4 and 5 also provide the RI parameter of the schemes. Table 4 indicates that the schemes 2, 5, and 6 can be adopted as the suitable methos for the Case 1 loading condition. Furthermore, for the Case 2 loading condition, Table 5 clearly shows that schemes 2, 5, and 6 outperform the other DR schemes for the form-finding of the structure.

The DR schemes obtained the same form-finding for the membrane structure subjected to two loading conditions.

**Table 4** Comparing the results of the DR schemes for the loading condition Case 1

Scheme	Number of iterations in each loading step loading				I^i	E^i_I	$T^i(s)$	E^i_T	RI
	1	2	3	4					
DRM 1	68	70	72	73	283	64	1.68	41.57	52.79
DRM 2	70	59	69	70	262	92	1.44	68.54	80.27
DRM 3	78	70	93	84	325	8	2.05	0	4
DRM 4	70	70	71	71	282	65.33	1.77	31.46	48.39
DRM 5	71	65	57	65	283	64	1.16	100	82
DRM 6	69	59	63	65	256	100	1.41	71.91	85.96
DRM 7	82	86	74	89	331	0	1.88	19.10	9.55

Table 5 Comparing the results of the DR schemes for the loading condition Case 2

Scheme	Number of iterations in each loading step loading				I^i	E_I^i	$T^i(s)$	E_T^i	RI
	1	2	3	4					
DRM 1	68	70	72	73	283	64	1.9	20.95	42.48
DRM 2	70	59	62	70	262	92	1.44	64.76	78.38
DRM 3	78	70	93	84	325	8	2.12	0	4
DRM 4	70	70	71	71	282	65.33	1.55	54.28	59.81
DRM 5	71	65	57	65	258	97.33	1.2	87.62	92.48
DRM 6	69	59	63	65	256	100	1.07	100	100
DRM 7	82	86	74	89	331	0	1.91	20.00	10
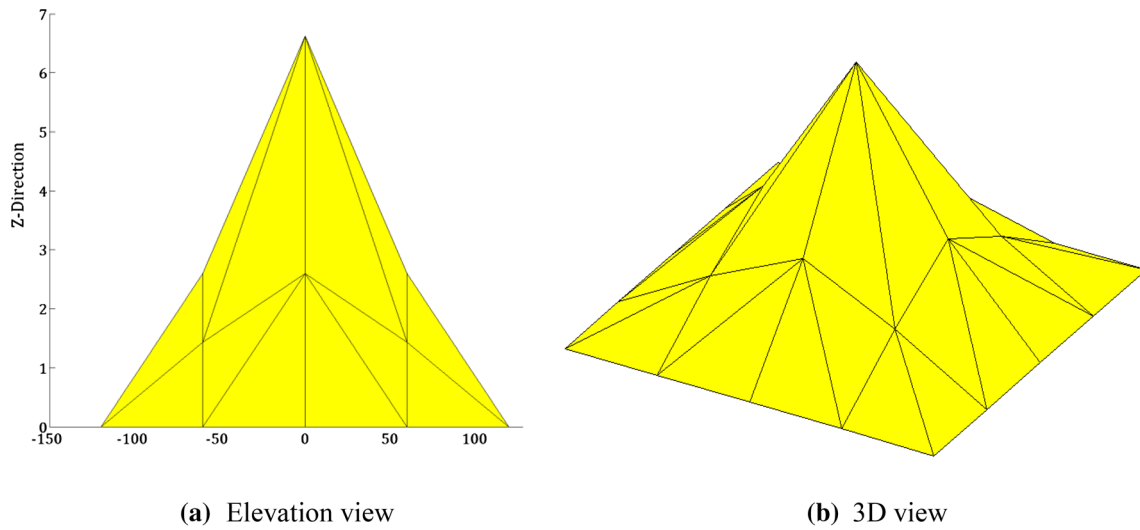
(a) Elevation view   **(b)** 3D view

Fig. 8 Form-finding model of the flat stretched membrane subjected to the loading condition Case 1

(a) Elevation view   **(b)** 3D view
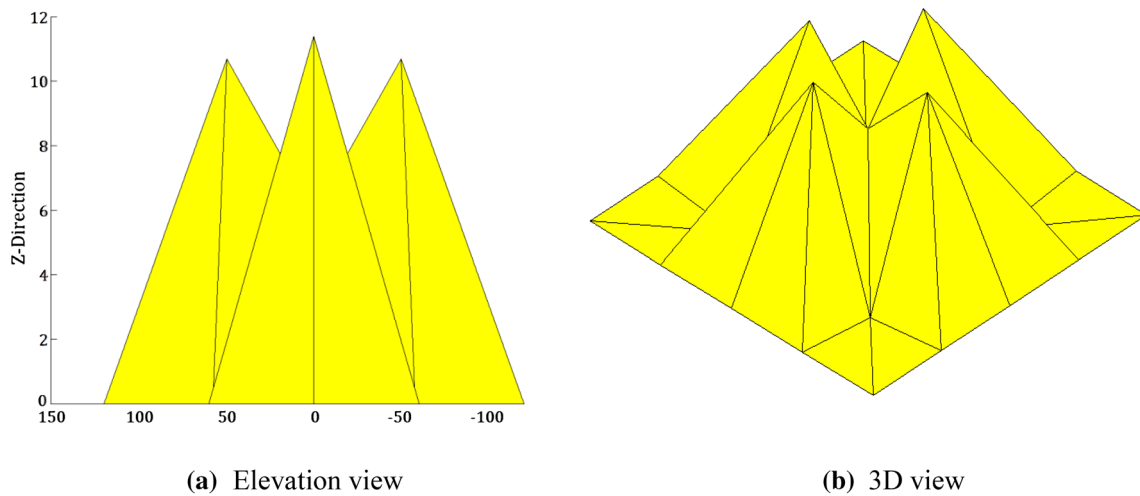
Fig. 9 Form-finding model of the flat stretched membrane subjected to the loading condition Case 2

Fig. 10 Kresge auditorium [31]

Figures 8 and 9 present the form-finding model of the flat stretched membrane subjected to the Case 1 and 2 loading conditions, respectively.

6.3 Practical example: Kresge auditorium

The efficiency of the DR schemes was further tested on a real structure. The roof of the Kresge auditorium at MIT, shown in Fig. 10, was constructed using a TMS and supported at three points. The shape of the building in plan was scaled from drawings, as well as the height of the parabolic openings along the borders.

These are the fixed nodes which were used in the DR schemes. While the plan dimensions and fixed elevations were based on the Kresge auditorium, the prescribed load and other parameters were chosen arbitrarily to generate a shape just for the purposes of visualization. The Young's modulus was considered as 10,000 ksi while the Poisson's ratio was 0.3. The thickness of this structure was taken as 0.01576 in. The initial prestress values in the warp and fill directions was assumed equal to 300 ksi. The load was applied at inner joints, which was equal to 10 kip.

Table 6 presents the comparison of the results of the DRM schemes in the form-finding procedure. The RI parameter of the schemes is also shown in Table 6.

As obvious from Table 6, the schemes 4, 3, and 2 are the best techniques. The schemes of DRM found the same form-finding for the membrane structure. The form-finding model of the Kresge auditorium is shown in Fig. 11.

7 Discussion

In order to evaluate and compare the performance of different *DR* schemes in the form-finding of TMSs, the present study calculated the RI average of each scheme by using the results of the examples. Table 7 provides the value of the RI average of the schemes.

Column G_i lists the grades of each scheme based on the RI average. Based on the value of the RI average, the schemes are graded from one to seven, as indicated in Table 7. According to the obtained grades, the higher ranking schemes with the good performance are schemes 2, 6, 4, and 3, respectively. Furthermore, scheme 1 (i.e., standard DRM) shows the worst performance.

Table 6 Comparing the results of the DR schemes for the form-finding of the Kresge auditorium

Scheme	Number of iterations in each loading step loading				I^i	E_I^i	$T^i(s)$	E_T^i	RI
	1	2	3	4					
DRM 1	126	127	137	173	563	0	1.92	39.53	19.77
DRM 2	58	89	81	100	328	74.84	1.56	67.44	71.14
DRM 3	49	83	89	101	322	76.75	1.24	92.25	84.49
DRM 4	49	54	60	81	249	100	1.14	100	100
DRM 5	118	121	130	165	534	9.24	1.85	44.96	27.09
DRM 6	106	113	124	160	503	19.11	2.35	6.21	12.65
DRM 7	72	98	150	215	535	8.98	2.43	0	4.46

Fig. 11 Form-finding model of the Kresge auditorium
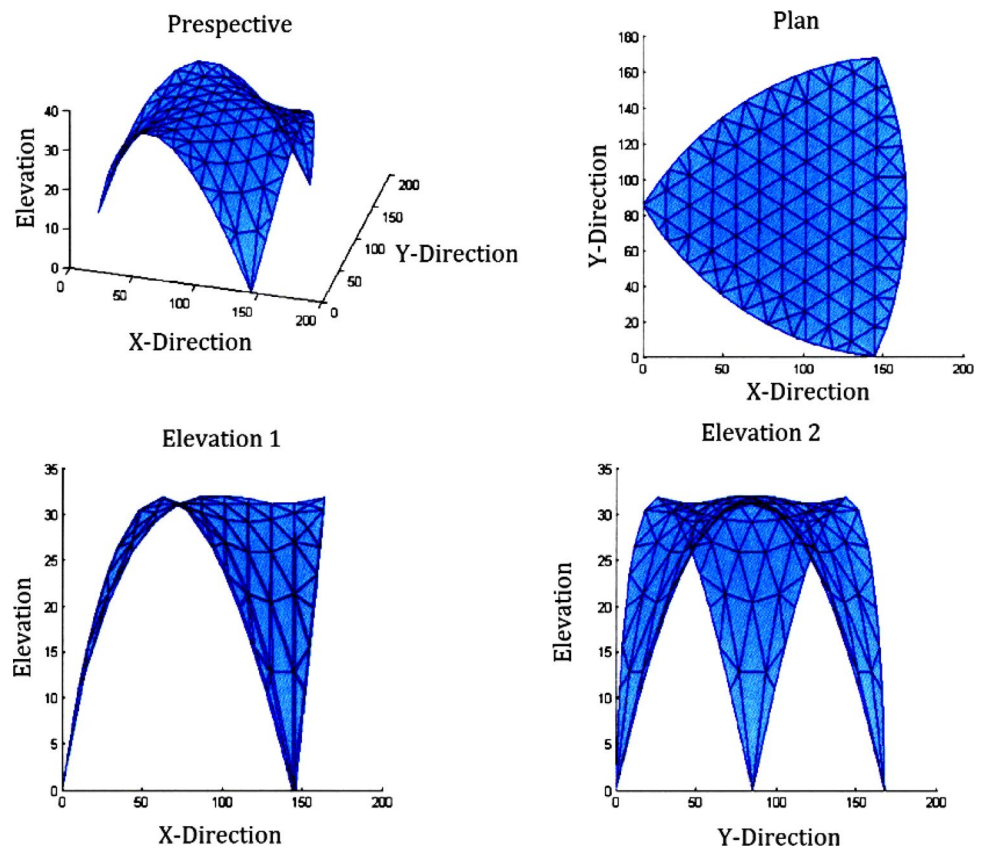
Table 7 Value of the RI average for the DR sachems

Scheme	Average of RI	G_i
DRM 1	29.792	7
DRM 2	72.516	1
DRM 3	39.284	5
DRM 4	59.1	3
DRM 5	58.858	4
DRM 6	67.616	2
DRM 7	33.902	6

- The results confirm that comparing both the total number of iterations and the overall duration of analysis is not appropriate for the purposes of the study. Hence, the proposed RI criterion instead of two criteria is adopted as the best criterion for assessing the efficiency of different DRMs.
- In the more cases of the study's examples, the results imply that the efficiency of the standard DRM (scheme 1) is not suitable in comparison with other schemes. Thus, the standard DRM can not be considered as a reliable approach in the TMS form-finding.
- Based on the obtained average of the RI, the schemes 2, 6, 4, and 3 have the high performance and can be recognized as the reliable schemes in the form-finding of TMSs.
- It is worth emphasizing that the best performance of the form-finding is obtained by the scheme 2 (i.e., the optimal time step approch proposed by Kadkhodayan et al. [27]).

8 Conclusions

The present study investigated the assessment of the efficiency of different DRMs which were used for the form-finding of TMSs. To achieve this purpose, the comparison was implemented based on the following criteria: the total number of iterations, the overall duration of the analysis, and a proposed reference index (RI). The current work introduced the proposed RI by combining the total number of iterations and the overall duration of analysis. Based on the results of the illustrative examples, the following conclusions were obtained:

Compliance with ethical standards

References

1. Lewis WJ (2003) Tension structures form and behavior. Thomas Telford, London
2. Dutta S, Ghosh S, Inamdar MM (2017) Reliability-based design optimization of frame-supported tensile membrane structures. J Risk Uncertainty Eng Syst Part A Civ Eng 3(2):1–11
3. Lewis WJ (2013) Modeling of fabric structures and associated design issues. J Archit Eng ASCE 19(2):81–88
4. Huntington CG (2013) Tensile fabric structures: design, analysis and construction. American Society of Civil Engineers, Reston
5. Linkwitz K (1999) Form finding by the direct approach and pertinent strategies for the conceptual design of pre-stressed and hanging structures. Int J Space Struct 14(2):73–87
6. Barnes MR (1994) Form and stress engineering of tension structures. Struct Eng Rev 6(3-4):175–202
7. Wakefield D (1999) Engineering analysis of tension structures: theory and practice. Eng Struct 21(8):680–690
8. Bletzinger KU, Ramm E (1999) A general finite element approach to the form finding of tensile structures by the updated reference strategy. Int J Space Struct 14(2):131–145
9. Kilian A, Ochsendorf J (2005) Particle-spring systems for structural form finding. J Int Assoc Shell Spatial Struct 46(148):77–84
10. Schek HJ (1974) The force density method for form finding and computations of general networks. Comput Methods Appl Mech Eng 3:115–134
11. Maurin B, Motro R (1998) The surface stress density method as a form-finding tool for tensile membranes. Eng Struct 20(8):712–719
12. Sanchez J, Serna MA, Morer P (2007) A multi-step force-density method and surface fitting approach for the preliminary shape design of tensile structures. Eng Struct 8:1966–1976
13. Ye J, Feng R, Zhou S, Tian J (2012) The modified force-density method for form-finding of membrane structures. Int J Steel Struct 12(3):299–310
14. Barnes MR (1999) Form finding and analysis of tension structures by dynamic relaxation. Int J Space Struct 14(2):89–104
15. Lewis WJ (2008) Computational form-finding methods for fabric structures. Eng Comput Mech 161(3):139–149
16. Alic V, Persson K (2016) Form finding with dynamic relaxation and isogeometric membrane elements. Comput Methods Appl Mech Eng 300:734–747
17. Roodsarabi M, Khatibinia M, Sarafrazi SR (2016) Hybrid of topological derivative-based level set method and isogeometric analysis for structural topology optimization. Steel Compos Struct 21(6):1287–1306
18. Khatibinia M, Roudsarabi M, Barati M (2018) Topology optimization of plane structures using binary level set method and isogeometric analysis. Int J Opt Civ Eng 8(2):209–226
19. Day AS (1965) An introduction to dynamic relaxation. The Engineer 219:218–221
20. Topping BHV, Ivanyi P (2007) Computer aided design of cable membrane structures. Saxe-Coburg Publications, Kippen
21. Rezaiee-Pajand M, Sarafrazi SR (2010) Nonlinear structural analysis using dynamic relaxation method with improved convergence rate. Int J Numer Methods Eng 7:627–654
22. Zhang LC, Yu TX (1989) Modified adaptive dynamic relaxation method and its application to elasticplastic bending and wrinkling of circular plates. Comput Struct 34:609–614
23. Rezaiee-Pajand M, Alamatian J (2008) Nonlinear dynamic analysis by dynamic relaxation method. Struct Eng Mech 28:549–570
24. Rezaiee-Pajand M, Sarafrazi SR, Rezaiee H (2012) Efficiency of dynamic relaxation methods in nonlinear analysis of truss and frame structures. Comput Struct 112-113:295–310
25. Rezaiee-Pajand M, Kadkhodayan M, Alamatian J (2012) Timestep selection for dynamic relaxation method. Mech Based Des Struc 40(1):42–72
26. Alamatian J, Hosseini-Nejad Goshik M (2016) An effcient explicit framework for determining the lowest structural buckling load using dynamic relaxation method. Mech Based Des Struc 45(4):1–12
27. Kadkhodayan M, Alamatian J, Turvey GJ (2008) A new fictitious time for the dynamic relaxation (DXDR) method. Int J Numer Methods Eng 74:996–1018
28. Sarafrazi SR (2012) Numerical integration for structural dynamic analysis. PhD Dissertation, Department of Civil Engineering, Ferdowsi University, Iran. (**in Persian**)
29. Zienkiewicz OC (1977) The finite element method. McGraw-Hill, New Jersey
30. Spillers WR, Schlogel M, Pilla D (1992) A simple membrane finite element. Comput Methods Appl Mech Eng 45(1):181–183
31. https://en.wikipedia.org/wiki/Kresge_Auditorium